The effect of façade curvature and surrounding building heights on pedestrian-level wind speeds in the City of London

Yujin Kim[1], George Jeronimidis[1], Hesham Ebrahim[1]

[1] Architectural Association, London, United Kingdom
yujin.kim@aaschool.ac.uk; george.jeronimidis@aaschool.ac.uk;
hesham.ebrahim@tetratech.com

Abstract. This paper analyses the effect of façade curvature with varying the surrounding building heights on pedestrian-level wind speeds and comfort for walking, using computational fluid dynamics. The case study focuses on 20 Fenchurch Street site in London as several complaints have risen in relation to high wind speeds, the cause of which is not thoroughly understood. The results of the simulation revealed that although the increase of surrounding building heights reduces overall pedestrian-level wind speeds for both curved existing and cuboid building, façade curvature impacts differently on winds, compared to the cuboid. Isolated curved and cuboid building would perform similarly with the exception of the northwest corner. However, introducing the existing surrounding buildings, the curved façade geometry would create larger area of walking discomfort compared to the cuboid geometry. When the height of the surrounding buildings is increased, both buildings would perform similarly with minor aerodynamic advantage to the curved-façade.

Keywords: Building Performance, Wind Microclimate, Tall Building, Surroundings, Pedestrian-level Wind Speeds.

1 Introduction

The previous literature and research of building aerodynamics did not explain the impact of curved façades on pedestrian-level winds (PLW). Many studies provided information about the relation of building geometry to PLW and comfort such as Druenen et al. (2019), Shirzadi and Tomingaga (2021) which investigated the effect of building geometry on PLW speeds and comfort. However, these studies were carried out with the perpendicular building façades. Moreover, Zhang et al. (2020) investigated the impact of a tall building on PLW comfort with an urban-like setting. They provided fundamental understanding of the influence of tall buildings on PLW comfort, however, the

simplified urban form was not representative of the complicated urban configurations in a real physical world. Furthermore, several studies replicated real urban conditions (Kubota et al., 2008; Tsichritzis & Nikolopoulou, 2019). They showed the relationship between urban parameters (plan area ratio and façade area ratio) and winds, however, the parameters were quite generalised and could not provide information as to which building geometry caused wind accelerations at pedestrian level. To address some of the limitations of previous studies, this paper has assessed the effect of façade curvature with surrounding building heights on PLW speeds and comfort for walking in a real urban condition. As walking is a main trip method, being recorded as the highest number of trips (5.5 – 6.7 million) from 2000 to 2018 among others (cycle, car, bus, underground, rail, etc.) in Greater London, according to Mayor of London (2019), this study focused on wind comfort for walking.

Computational Fluid Dynamics (CFD) simulations were used to run four conditions: 1) Isolated building, 2) Real urban context with the existing surrounding buildings, and 3) A building surrounded by the same existing buildings with increased height up to 50% and 4) 100% of the target building. South-westerly wind direction (225°) was the input as it is the prevailing wind direction for London with a probability of 26.5% in winter. As this study focuses on PLW comfort, wind speed is considered as the main environmental parameter that is relevant to the mechanical effect of winds. Two parameters, the average and threshold wind speed ratio for walking comfort, were represented to assess the effect of façade curvature and surrounding building heights on PLW speeds.

2 Methodology

2.1 Computational Setup

The CFD simulations were carried out using OpenFOAM (v.9) software. Reynolds-averaged simulation with the k-ϵ realizable turbulent model was implemented with the semi-implicit method for pressure-linked equations algorithm. Computational domain was setup in an octagonal shape (Figure 1).

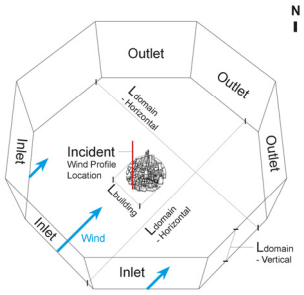

Figure 1. Computational domain

In order to avoid artificial acceleration by blockage due to computational walls, the dimensions of the domain were setup with a directional blockage ratio that is less than 3% (Blocken, 2015). An atmospheric boundary layer profile was setup as an inlet with aerodynamic roughness length (Z_0) of 2m (Wieringa, 1992) reference height (Z_∞) is 518m (Davenport, 1963), and reference wind speed (U_∞) is 10 m/s based on the best practice standards of external aerodynamic studies. From the empty domain, the profiles of wind speed and turbulent kinetic energy (k) at the incident location (refer to Figure 1) are represented in Figure 2. The reference wind speed, U_∞ from the inlet maintained its shape with potential flow reaching 10m/s (rounded to the nearest ones) is also indicated at 518m height as shown in Figure 2.

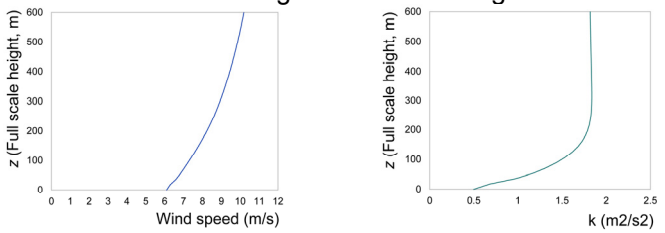

a. Wind speed profile b. Kinetic energy (k) profile

Figure 2. The profiles of wind speed (a), and kinetic energy profile (b) at the incident location at an empty computational domain

The domain was discretised into a total of 19.6 million cells (Figure 3).

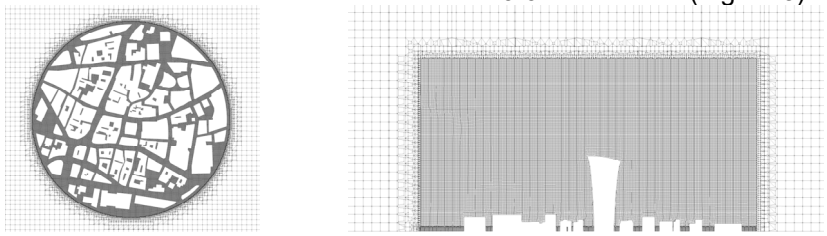

Plan View Section View

Figure 3. Structural mesh

The CFD results were validated against wind tunnel measurements made by Architectural Institute of Japan (Yoshie et al., 2007) and on-site monitoring with a mobile weather station.

2.2 Test Geometries and Urban Forms

To analyse the effect of building heights on pedestrian-level wind speeds, three-dimensional computational models were setup as follows:

1) An isolated building condition with the existing (convex/concave) and a cuboid target building as shown in Figure 4. This simulation will serve as the baseline without the influence of surrounding buildings characterize the pure aerodynamic performance of each geometry.

2) The existing and cuboid target building with the existing urban context of CoL (see Figure 5).
3) The existing and cuboid building with increased surrounding building height to 50% (see Figure 6) and 100% of the target building (see Figure 7).

Figure 4. Existing (left) and cuboid target building (right)

Figure 5. Existing (left) and cuboid target building (right) with existing surrounding buildings

Figure 6. Existing (left) and cuboid target building (right) with surrounding buildings at 50% height

Figure 7. Existing (left) and cuboid target building (right) with surrounding buildings at 100% height (bottom)

As this study focuses on the effect of buildings height on PLW speeds, detailed parts of the buildings, such as canopies, podiums, and roof shapes were simplified for the scope of this study.

2.3 Buildings and Urban Configuration Performance Analysis Technique

To assess the wind speed at pedestrian level areas surrounding the main building, five zones were chosen as shown in Figure 8.

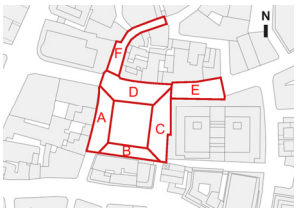

Figure 8. Analysis zones A – F

All wind speeds are represented as ratios (U) in accordant with Equation 1:

$$U = \frac{U_0}{U_\infty} \quad (1)$$

U_0 (m/s) is defined as the local wind speed at 1.5m above ground level and U_∞ is the reference wind speed, 10 m/s at 518m above ground level.

2.4 Average (U_{ave}) and threshold wind speed ratio for walking (U_{tw})

To assess U, two parameters were used, the average (U_{ave}) and the area (%) that exceeds threshold wind speed ratio for walking (U_{tw}). U_{ave} is the mean value of U at 1.5m above ground level. U_{tw} is defined as the threshold of U that can cause discomfort for walking. For this study, U_{tw} is quantified using the Weibull distribution obtained from the City of London (CoL) wind microclimate guidelines (City of London and RWDI, 2019).

The 36 Weibull parameters obtained from the CoL guidelines were initially converted to 8 for this study (see Table 1) where parameters *p, c,* and *k* are the probability, scale and shape factors respectively. It should be noted that this study shown in the present paper is a part of a larger investigation that assess a building and the urban form on all 8 wind directions instead of 36 directions, hence the conversion was made.

Table 1. Weibull parameters in winter for 8 wind direction (45° increments)

Direction	N	NE	E	SE	S	SW	W	NW
p	0.081	0.094	0.086	0.064	0.134	0.265	0.193	0.087
c	4.73	6.01	6.40	5.23	6.65	7.60	6.75	5.24
k	1.54	1.93	2.02	1.97	1.83	2.00	1.72	1.61

Moreover, to calculate U_{tw} for this study, the equation for PLW comfort (2) was used:

$$f(x) = P \cdot e^{-\left(\frac{x}{U_{tw} \cdot 1.42 \cdot c}\right)^k} \quad (2)$$

Where $f(x)$ is the probability of exceedance for the season, x is wind speed threshold value for the activity. Since this study is concerned with walking that is when 8 m/s mean velocity exceeds 5% of the time, it is considered uncomfortable according to the CoL Guidelines. Therefore, $f(x)$ is capped to 0.05 (i.e. 5%) and x is 8 (m/s). U is wind speed ratio (refer to Equation 1), 1.42 is the reference height scale factor that is interpolated in accordance with the CoL Guidelines to match the reference height (518m) used in the simulations. Note that $f(x)$ is the sum of probability considering all wind directions (i.e. all 8

angles). However, this study focuses on the prevailing SW wind direction only and therefore should the probability exceed 5% it would indicate discomfort without testing other angles. The contribution of other angles would increase the probability and worsen the comfort which is important in more detailed investigations. When the parameters for SW in Table 1 are substituted into Equation 2, and the equation is solved for U_{tw} would therefore be:

$$U_{tw} = 8 \cdot (1.42 \cdot 7.60 \cdot \sqrt{-\log_e \frac{0.05}{0.265}})^{-1} \quad (3)$$

Hence, 0.57 (rounded to the nearest hundredth) is U_{tw} that can cause walking discomfort from one wind direction.

3 Results

3.1 Average wind speed ratio (U_{ave}) and PLW patterns

The average wind speed ratio (U_{ave}) for zones A – F are represented in Figures 9. In the isolated tall building condition, overall U_{ave} of the existing and cuboid buildings show similar values. However, at zone A, U_{ave} of the existing building is slightly higher than the cuboid building.

Figure 10 shows the contours of wind speed ratio (U) at 1.5m above ground level. Higher U appears to occupy a larger area of zone A for the existing building due to the convex façade compared to the cuboid. In addition, a larger wake occurs in zones B and C for the existing building than the cuboid (Figure 10). These variations in velocities are due to the western convex façade of the existing building which pushes the fast-moving air slightly farther to the north west direction than the cuboid thus creating a larger wake.

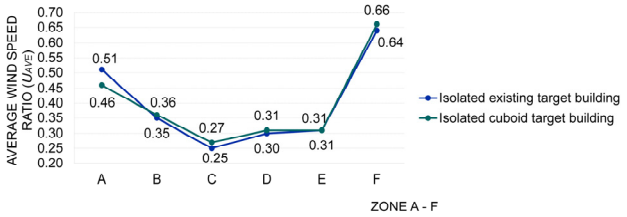

Figure 9. U_{ave} at pedestrian level with the isolate existing and cuboid target building

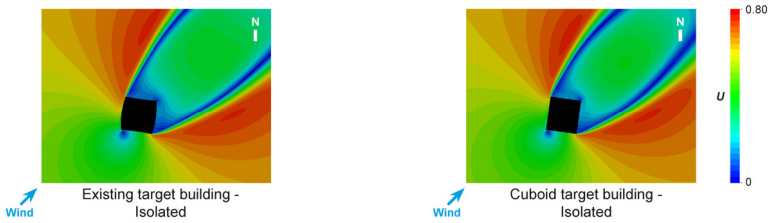

Figure 10. U at pedestrian level by an isolated existing and cuboid building

With the existing surrounding buildings introduced, the existing target building accelerated the wind marginally more than the cuboid building at zones A (the westerly frontal area), C, D and F (the wake area of the buildings) (Figure 11).

The underlining accelerations at the corners remained visible at zones C and D for both the existing and cuboid buildings (Figure 12). These accelerations were due to the convex angle of the western façade of the existing target building which created a narrower channel for the wind thereby causing higher corner acceleration with a stronger venturi effect than the cuboid (where the channel remained uniform). The curvature of the south façade of the existing target building also caused a stronger flow separation at the south-eastern corner creating a longer stream of higher-speed winds at zone C than the cuboid building.

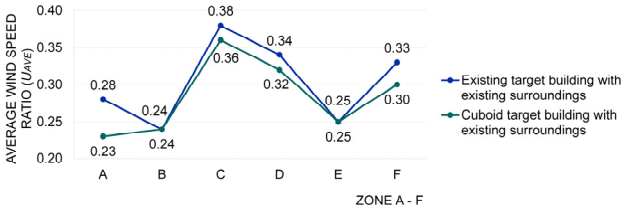

Figure 11. U_{ave} at pedestrian level with the existing and cuboid target building with existing surrounding buildings

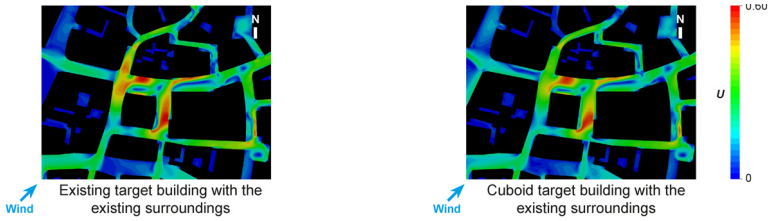

Figure 12. U at pedestrian level in existing and cuboid target building with existing surrounding buildings

When target buildings were surrounded by buildings of 50% height, the wind speed became higher for the cuboid compared to the existing target building at B, D, E, and F although at zone B and E the differences of wind speed were minor between the two buildings (Figure 13). At zone A, the wind speed was slightly higher for the existing target building compared to the cuboid.

Figure 14 shows the velocity contours for the 50% height case. Due to the increase in surrounding buildings height to 50% of the target building, the fast-moving wind flows above buildings to the west of the target reducing the amount of high speed winds reaching pedestrian level. Thereby, the venturi effect minimised compared to the existing case condition where the surrounding buildings were shorter (see Figure 12). Moreover, the convex geometry in the direction of the flow is more streamlined with lesser frontal area facing the wind direction compared to the cuboid. As such less wind is being channelled to

pedestrian level to the west of the target building. This effect is, however, reversed on the southern façade as the flow separates at the south-eastern corner and interacts with the western elevation of the building to the east before accelerating to ground level.

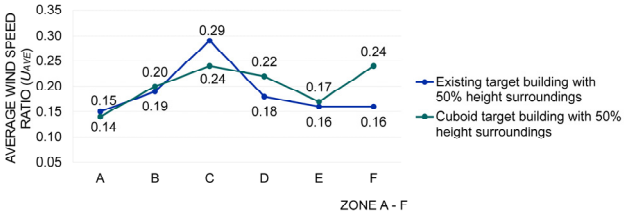

Figure 13. U_{ave} at pedestrian level with the existing and cuboid target building surrounded by 50% height buildings

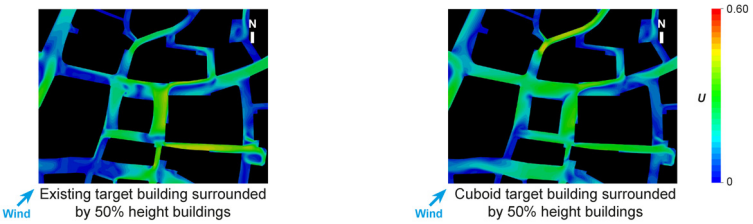

Figure 14. U at pedestrian level with existing and cuboid target building surrounded by 50% height buildings

When the surrounding buildings are the same height of the existing building (160m tall), overall, the cuboid-shaped tall building would generate slightly faster winds at pedestrian level, except for zone F (Figure 15).

Looking at the U patterns at pedestrian level shown in Figure 16, the sheltering effect provided by the surroundings would reduce the overall wind speed. As the overall wind speed decreases, both geometries generated similar flow pattern at zones A to F. However, the cuboid building generates slightly higher-speed winds than the existing target building as the upper part of the target building (defined by the convex shape at the east and west) reduced the amount of high wind speeds from moving down to pedestrian level in comparison to the cuboid.

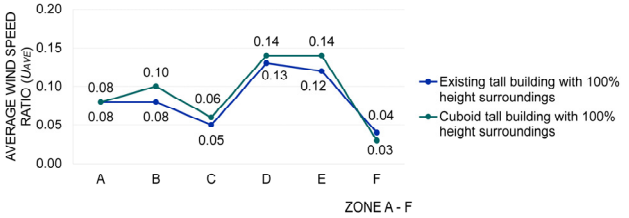

Figure 15. U_{ave} at pedestrian level with the existing and cuboid target building surrounded by 100% height buildings

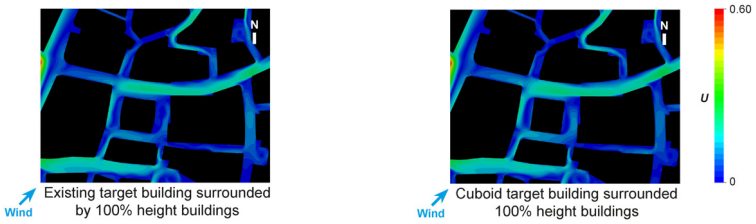

Figure 16. U at pedestrian level with existing and cuboid target building surrounded by 100% height buildings

Figure 17 shows the summary of results, representing the relationship between façade curvature of a target building with surrounding building heights and PLW speeds. It shows the trends that as the heights of surrounding buildings become taller (without the surroundings, with the existing, 50%, and 100% height surroundings), the overall wind speeds decreased over the zone A – F, except for zone C and D between the isolated and existing surrounding conditions. From this trend, however, the curved existing and cuboid target building generated the different wind speeds as follows: 1) In the isolated condition, the existing target building performed marginally better than the cuboid at B, C, D, E, and F with generating slightly lower-wind speeds. 2) With the existing surroundings, the cuboid worked better at A, C, D, and F. 3) With the surrounding buildings at 50% height of the target building, the existing target building would be favourable to a slight extent than the cuboid at B, D, E, and F. 4) With the surrounding height of 100% of the target building: the existing target building had minor advantages with creating slightly lower-moving flows than the cuboid at B, C, D, and E.

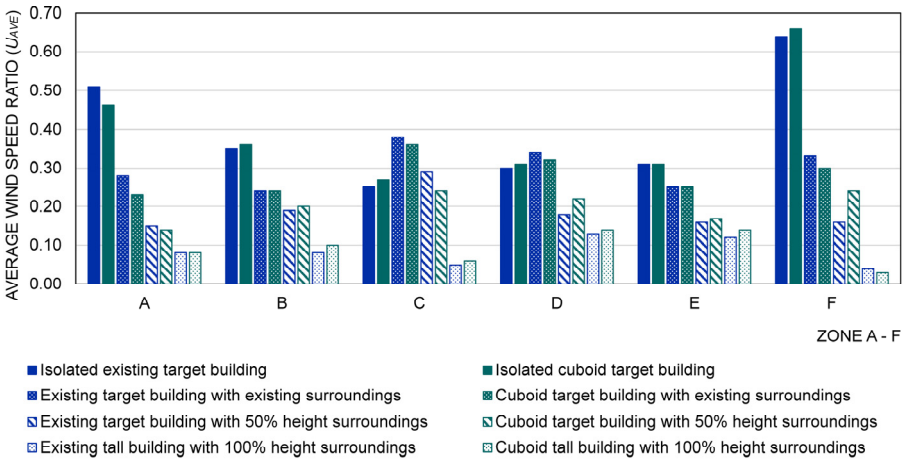

Figure 17. The summary of the results showing the relationship between façade curvature with the surrounding building heights and U_{ave} at 1.5m above ground level of zone A - F

3.2 Threshold U for walking discomfort (U_{tw})

Figure 18 indicate the walking discomfort zone for each tested building in isolation. At the northwest corner, the existing building generates a larger walking discomfort zone in comparison to the cuboid. This is because the convex angle of the west façade creates higher wind speeds than the perpendicular angle. However, the concave angle of the south façade of the existing building performed similarly to the perpendicular angle of the cuboid, having similar discomfort zone. The free shear area of both buildings show similar patterns.

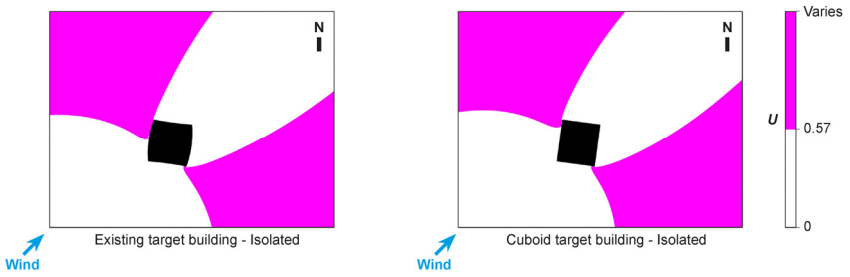

Figure 18. Areas over U_{tw} (0.57) with the existing (left) and cuboid (right) target building in the isolated condition

Introducing existing surroundings created different areas of walking discomfort between the existing and cuboid target building (see Figure 19). Overall, the walking discomfort areas decreased in comparison to the isolated condition. However, the cuboid performed better, inducing the smaller area of walking discomfort.

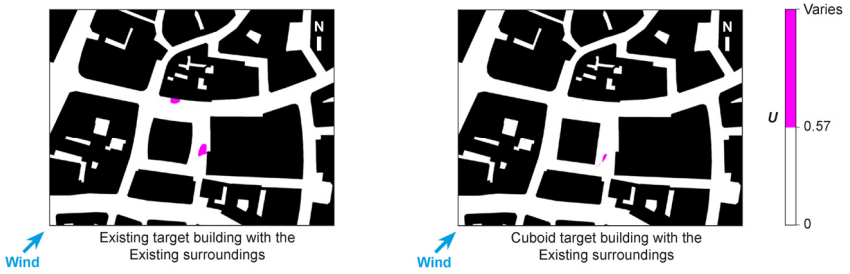

Figure 19. Areas over U_{tw} (0.57) with the existing (left) and cuboid (right) target building with the existing surroundings

When the height of the surrounding buildings is 50% and 100% of the existing building, all discomfort zones are eliminated.

4 Conclusions and Contributions

This paper presents the effect of façade curvature with surrounding building heights on pedestrian-level winds by CFD simulations. The summary of new findings are as follows: although overall PLW speeds are decreased as the surrounding building heights become taller, the existing and cuboid target building generate different PLW speeds, based on the curvature of building facades. In the isolated condition, the existing target building performs marginally better than the cuboid as the convex façade rather pushes away the fast-moving winds and creates larger wake zones. When the existing surrounding buildings are introduced, the cuboid works better. This is because the curvature of the existing target building causes higher corner acceleration due to the stronger venturi effect at the north west corner, and the longer stream of higher-speed winds at the south-eastern corner because of the flow separation than the cuboid. As the heights of surrounding buildings become 50% height of the target building, the venturi effects are minimised due to the overflow of the fast moving winds, compared to the existing condition. The curved existing target building would be slightly favourable than the cuboid. This is because the convex facade at the west side makes the frontal area to be reduced in comparison to the cuboid, and thereby, less winds were channelled. But this effect is reversed at the south façade as the flow separation occurred at the south-eastern corner. When the surrounding buildings are the same height as the existing building, the existing target building shows minor advantage because the convex façades make less amount of fast-moving winds to reach to the pedestrian level. Thus, slightly lower-speed winds occurs compared to the cuboid.

Examining the effect of façade curvature with surrounding building heights on wind comfort for walking, in the isolated building condition, the convex geometry of the existing target building at the west side generates larger discomfort zone than the cuboid. With the existing surroundings, the cuboid worked better, creating less area of discomfort zone for walking than the existing target building. As the surrounding building heights become 50% and 100% of the target building, discomfort zones are eliminated.

Whilst this paper focused on the CoL, as the study examined the interactions between façade curvature and surrounding building heights, it is relevant to the building in the other cities, in particular, of which urban forms are not in grid layouts but in curvy shapes and close proximities. The investigations in this paper is a part of the study that covers the wind effects, affected by various geometries of an isolated building (cuboid, pyramid, constant, and inconstant-angled facades) and the tall buildings in an urban context.

References

Blocken, B. (2015). Computational Fluid Dynamics for urban physics: Importance, scales, possibilities, limitations and ten tips and tricks towards accurate and reliable

simulations. Building and Environment, 91, 219-245. https://doi.org/10.1016/j.buildenv.2015.02.015

City of London and RWDI. (October 1, 2019). City of London Wind Microclimate Guidelines. Retrieved February 1, 2021, from https://www.cityoflondon.gov.uk/assets/Services-Environment/wind-microclimate-guidelines.pdf

Davenport, A. G. (1963). The relationship of wind structure to wind loading. Wind effects on buildings and structures conference (pp. 54-111). National Physical Laboratory. Retrieved September 13, 2022, from https://www.aivc.org/resource/relationship-wind-structure-wind-loading

Druenen, T.V., Hooff, T.V., Montazeri, H., & Blocken B. (2019). CFD evaluation of building geometry modifications to reduce pedestrian-level wind speed. Build. Environ., 163 (106293). https://doi:10.1016/j.buildenv.2019.106293

Kubota, T., Miura, M., Tominaga, Y., & Mochida, A. (2008). Wind tunnel tests on the relationship between building density and pedestrian-level wind velocity: Development of guidelines for realizing acceptable wind environment in residential neighborhoods. Building and Environment, 43 (10), 1699-1708. https://doi.org/10.1016/j.buildenv.2007.10.015

Mayor of London. (2019). Travel in London, Report 12. Retrieved February 8, 2022, from https://content.tfl.gov.uk/travel-in-london-report-12.pdf

Shirzadi, M. & Tominaga, Y. (2021). Multi-fidelity shape optimization methodology for pedestrian-level wind environment. Build. Environ., 204 (108076). https://doi:10.1016/j.buildenv.2021.108076

The OpenFOAM Foundation. (2022). OpenFOAM (version 9) [Computer software]. https://openfoam.org/version/9/

Tsichritzis, L. & Nikolopoulou, M. (2019). The effect of building height and façade area ratio on pedestrian wind comfort of London. Journal of Wind Engineering & Industrial Aerodynamics, 191, 63-75. https://doi.org/10.1016/j.jweia.2019.05.021

Yoshie, R., Mochida, A., Tominaga Y., Kataoka, H., Harimoto, K., Nozu, T., & Shirasawa, T. (2007). Cooperative project for CFD prediction of pedestrian wind environment in the Architectural Institute of Japan. Journal of Wind Engineering and Industrial Aerodynamics, 95, 1551-1578. https://doi.org/10.1016/j.jweia.2007.0

Wieringa, J. (1992). Updating the Davenport roughness classification. Journal of Wind Engineering and Industrial Aerodynamics, 41, 1-3, 357-368. https://doi.org/10.1016/0167-6105(92)90434-C

Zhang, X., Weerasuriya, A.U., Zhang, X., Tse, K.T., Lu, B., Li, C.Y., & Liu, C. (2020). Pedestrian wind comfort near a super-tall building with various configurations in an urban-like setting. BUILD SIMUL, 13, 1385-1408. https://doi.org/10.1007/s12273-020-0658-6